© 2017. Published by The Company of Biologists Ltd | Development (2017) 144, 1065-1071 doi:10.1242/dev.145045

Derivation of a robust mouse mammary organoid system for studying tissue dynamics

Paul R. Jamieson[1,2,*], Johanna F. Dekkers[1,2,*], Anne C. Rios[1,2], Nai Yang Fu[1,2], Geoffrey J. Lindeman[1,3,4] and Jane E. Visvader[1,2,‡]

ABSTRACT

Advances in stem cell research have enabled the generation of 'mini organs' or organoids that recapitulate phenotypic traits of the original biological specimen. Although organoids have been demonstrated for multiple organ systems, there are more limited options for studying mouse mammary gland formation *in vitro*. Here, we have built upon previously described culture assays to define culture conditions that enable the efficient generation of clonal organoid structures from single sorted basal mammary epithelial cells (MECs). Analysis of Confetti-reporter mice revealed the formation of uni-colored structures and thus the clonal nature of these organoids. High-resolution 3D imaging demonstrated that basal cell-derived complex organoids comprised an inner compartment of polarized luminal cells with milk-producing capacity and an outer network of elongated myoepithelial cells. Conversely, structures generated from luminal MECs rarely contained basal/myoepithelial cells. Moreover, flow cytometry and 3D microscopy of organoids generated from lineage-specific reporter mice established the bipotent capacity of basal cells and the restricted potential of luminal cells. In summary, we describe optimized *in vitro* conditions for the efficient generation of mouse mammary organoids that recapitulate features of mammary tissue architecture and function, and can be applied to understand tissue dynamics and cell-fate decisions.

KEY WORDS: 3D imaging, Mammary organoids, Clonality, *In vitro* lineage tracing, Multicolor reporter mice, Stem/progenitor cells

INTRODUCTION

The mammary epithelium is highly dynamic in nature and undergoes dramatic changes in tissue architecture during its postnatal development (Watson and Khaled, 2008). Ductal morphogenesis in puberty leads to the formation of a highly elaborate ductal tree that fills the entire fat pad, with lateral branching accompanying estrus cycling during the adult stage. Morphological changes in pregnancy are characterized by the generation of milk-producing alveolar units. The bilayered ductal tree comprises two primary lineages of cells, luminal and myoepithelial, the latter of which lie in a basal position. Extensive clonal colony-forming assays, transplantation assays and *in vivo* lineage-tracing studies have been carried out to understand the relationship between the different epithelial lineages, providing evidence for the existence of both bipotent and unipotent stem cells in the adult mammary gland (Rios et al., 2014; Shackleton et al., 2006; Stingl et al., 2006; van Amerongen et al., 2012; Van Keymeulen et al., 2011; Wang et al., 2015). Further characterization of the cellular heterogeneity within the mammary gland is important for deciphering mechanisms that predispose cells to oncogenesis.

In recent years, the advent of innovative methods to rebuild 'mini organs' or organoids *in vitro* has provided exciting new possibilities for studying tissue development and disease (Clevers, 2016). Sato and colleagues pioneered this method for intestinal stem cells and showed that a single stem cell could form 3D structures that recapitulated features of normal tissue architecture (Sato et al., 2011a,b, 2009). This organoid system was subsequently adapted for other organs, including the liver, prostate and pancreas (Boj et al., 2015; Huch et al., 2013; Karthaus et al., 2014). In the context of the mammary gland, most studies have relied on traditional colony-forming assays (Shackleton et al., 2006; Stingl et al., 2006, 1998). Development of mammary organoid models is currently an area of intense interest. Several recent studies on mouse or human breast epithelial cells have used advanced culture medium and 3D scaffolds for the formation of budding or TDLU-like structures that comprise luminal and basal cells layered in the correct orientation (Jardé et al., 2016; Linnemann et al., 2015; Panciera et al., 2016; Sokol et al., 2016; Zhang et al., 2016a,b). In this study, we have established conditions that enable robust formation of organoids from single sorted mouse basal and luminal epithelial cells, with high efficiency and reproducibility. Basal cells could form bi-lineage organoids within 2 weeks at a frequency of 20%. Characterization of these structures using high-resolution 3D imaging technology (Rios et al., 2014, 2016) and lineage-specific mouse reporter models has provided novel insights into the cellular dynamics of organoid formation.

RESULTS AND DISCUSSION

Efficient generation of clonal organoids from single sorted mammary epithelial cells

To study the formation of mammary epithelial organoids *in vitro*, mouse mammary epithelial cells (MECs) were isolated and sorted on the basis of their CD24 and CD29 expression profile (Fig. 1A) (Shackleton et al., 2006). Basal or luminal cells were plated in basement membrane extract (BME), a 3D support that mimics the *in vivo* extracellular matrix (Huch et al., 2013; van de Wetering et al., 2015), and then cultured in media containing factors previously used for organotypic cultures of both non-mammary (e.g. intestine and prostate) and mammary origin (Karthaus et al., 2014; Sato et al., 2009; Stingl et al., 2001). Activation of the Wnt pathway by Wnt3a and R-spondin 2, which is important for stem cell maintenance in many tissues (Kim et al., 2008; Zeng and Nusse,

[1]Stem Cells and Cancer Division, The Walter and Eliza Hall Institute of Medical Research, Parkville, Victoria 3052, Australia. [2]Department of Medical Biology, The University of Melbourne, Parkville, Victoria 3010, Australia. [3]Familial Cancer Centre and Department of Medical Oncology, The Royal Melbourne Hospital, Parkville, Victoria 3050, Australia. [4]Department of Medicine, The University of Melbourne, Parkville, Victoria 3010, Australia.
*These authors contributed equally to this work

‡Author for correspondence (visvader@wehi.edu.au)

J.E.V., 0000-0001-9173-6977

Received 22 September 2016; Accepted 30 November 2016

Development (2017) 144, 1065-1071 doi:10.1242/dev.145045

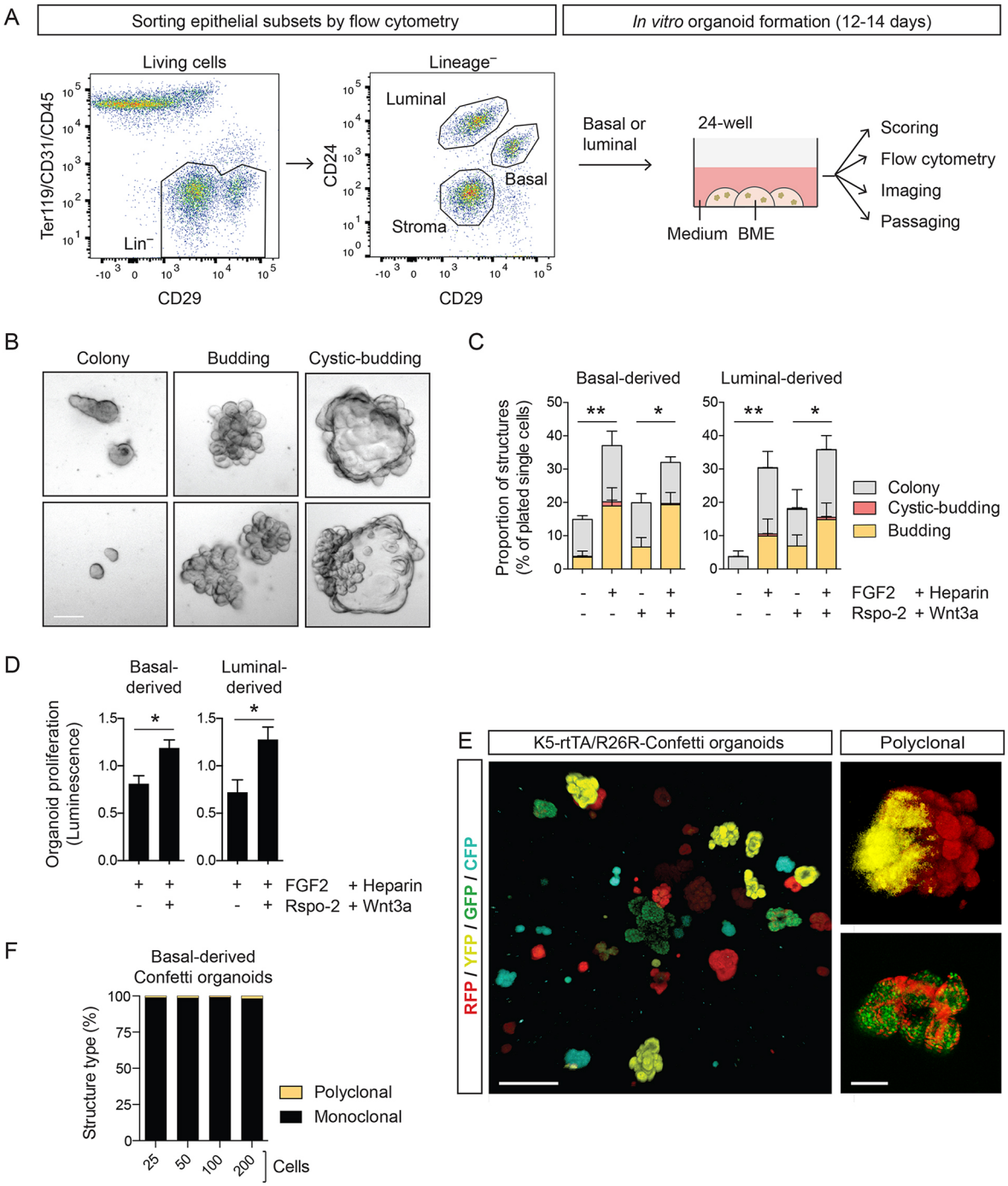

Fig. 1. Efficient generation of clonal organoids from single sorted MECs. (A) Schematic overview of generation of organoids from flow cytometry-sorted basal and luminal cells of the mouse mammary gland. BME, basement membrane extract; Lin⁻, lineage negative. (B) Representative examples of 2-week-old organoids grown from single basal cells. Scale bar: 100 µm. (C) Quantification of different structure types cultured with or without addition of FGF2/heparin or Rspo2/Wnt3a over 12-14 days. Structures generated from 200-400 single cells (25 cells/10 µl BME) were quantified per condition. Asterisks indicate significant differences between the total number of structures. *P<0.05; **P<0.01 (Student's t-test). Data are mean±s.e.m.; basal, n=3 or 4 experiments; luminal, n=4 experiments. (D) Quantification of organoid proliferation in 12- to 14-day-old cultures in the presence or absence of Rspo2/Wnt3a, as measured by the cell titer-glow cell viability assay. Values were normalized to the average of the two conditions per experiment. Data are mean±s.e.m. *P<0.05 (Student's t-test) (n=3 experiments). (E) Left panel: 3D confocal microscopy images of organoids generated from single epithelial cells from a K5-rtTA/TetO-cre/R26R-Confetti mouse, seeded at 200 cells per 10 µl BME. Scale bar: 300 µm. Right panels: examples of polyclonal Confetti-fluorescent organoids. Scale bar: 50 µm. (F) Quantification of monoclonal and polyclonal organoids derived from single cells plated at varying densities. Per cell density, 70-250 structures were counted (representative data for two experiments).

2010), and the branching-stimulating factors FGF2 and heparin (Ewald et al., 2008; Mroue and Bissell, 2013), have been shown to be important for enhancing the formation of organoid-like structures *in vitro*.

To establish the conditions for obtaining robust mouse mammary organoids, we tested a variety of media and growth factors, including Wnt3a, R-spondin 2, FGF2 and heparin. Different types of organoid structures were generated from basal or luminal cells,

Development (2017) 144, 1065-1071 doi:10.1242/dev.145045

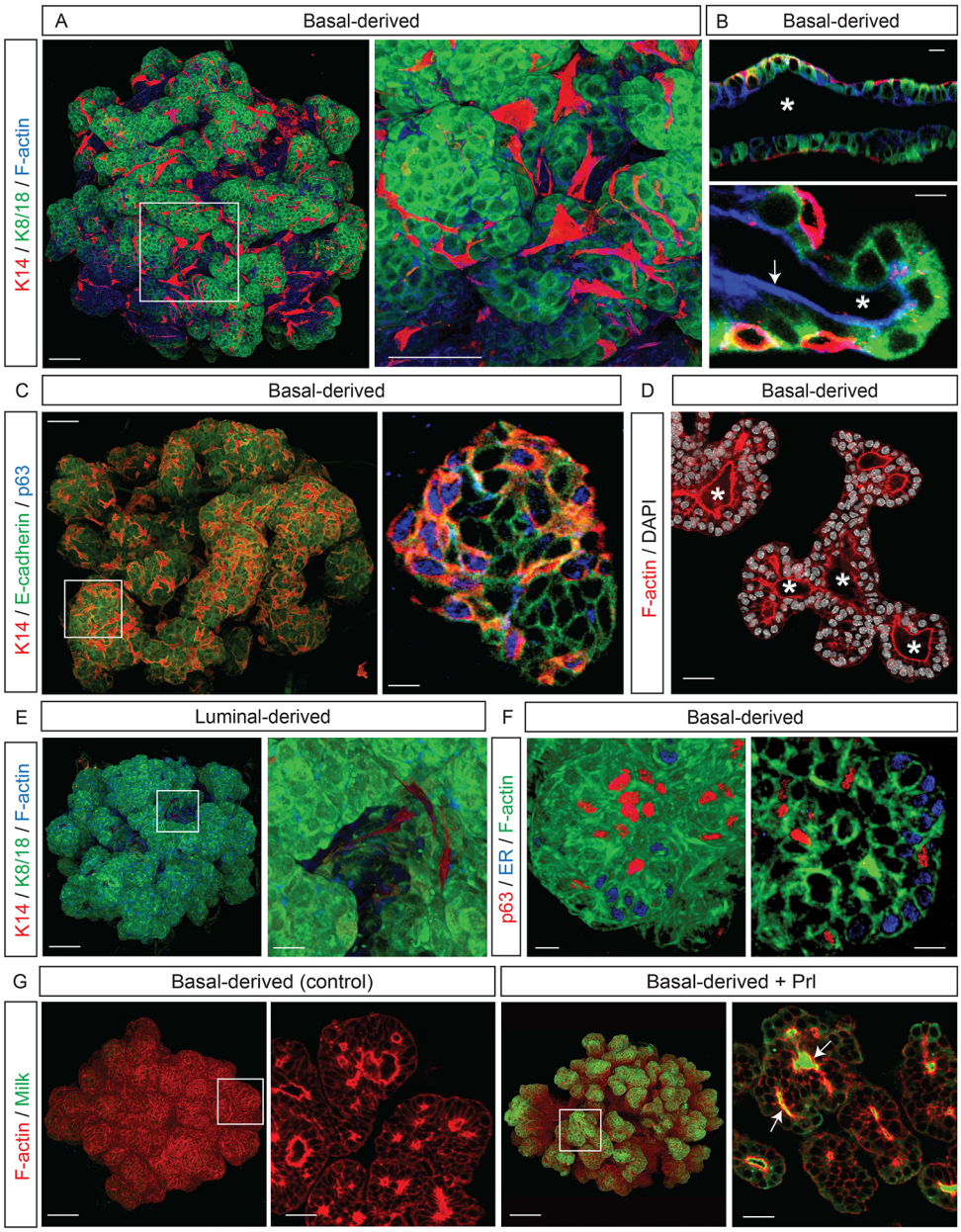

Fig. 2. Characterization of organoid architecture using 3D confocal imaging. (A,B) Whole-mount 3D confocal image and an enlarged section (A) or optical sections (B) of basal- derived organoids, labeled for K8/18, K14 and F-actin. White arrow indicates the apical membrane of luminal cells; white asterisks indicate the organoid lumen. Scale bars: 25 µm in A; 5 µm in B. (C) A whole-mount 3D confocal image and an optical section of a basal-derived organoid labeled for E-cadherin, p63 and K14. Scale bars: 30 µm (whole mount) and 8 µm (section). (D) Optical section of a basal-derived organoid labeled for F-actin and DAPI. White asterisks indicate the organoid lumen. Scale bar: 20 µm. (E) Whole-mount 3D confocal image and an enlarged section of a luminal-derived organoid labeled for K8/18, K14 and F-actin. Scale bars: 35 µm (whole mount); 10 µm (section). (F) Enlarged region of a whole-mount 3D confocal image and an optical section of basal-derived organoids labeled for ER, p63 and F-actin. Scale bars: 8 µm. (G) Whole-mount 3D confocal images and enlarged optical sections of basal-derived organoids with or without prolactin (Prl) stimulation, labeled for F-actin and milk. Scale bars: 50 µm (whole mounts); 20 µm (sections). Images are representative of two or three experiments; three to six organoids were imaged per experiment.

categorized as ‘colony’, ‘budding’ or ‘cystic-budding’ (Fig. 1B). Plating at a low cell density (25 cells/drop), we observed that up to 20% (basal) or 15% (luminal) of cells formed complex budding/branching or cystic-budding organoids, and up to ∼37% (basal and luminal) generated any type of structure (Fig. 1C). These structures differed from the round solid colonies generally formed from basal cells and from the cystic colonies generated by luminal cells in traditional Matrigel colony-forming assays (Shackleton et al., 2006; Stingl et al., 2006). Addition of FGF2 and heparin enhanced basal cell-derived organoid formation, and appeared to be crucial for the formation of budding organoids from luminal cells (Fig. 1C). Activation of the Wnt3a pathway did not affect organoid number or phenotype (Fig. 1C), but increased proliferation of organoids derived from either basal or luminal cells (Fig. 1D). ROCK inhibition using Y27632 for the first 3 days of culture substantially increased ‘budding’ organoid formation (Fig. S1A-C), in line with its role in reducing dissociation-induced apoptosis of single cells (Sato et al., 2009; Watanabe et al., 2007). Furthermore, proliferation was enhanced by progesterone and β-estradiol, thus indicating that the organoids are responsive to hormones (Fig. S1D).

Overall, the efficiency of formation of branching organoids from freshly sorted single cells was higher than that previously reported for mouse organoids (∼4%) (Zhang et al., 2016a) or human TDLU-like structures (∼0.2%) (Linnemann et al., 2015; Sokol et al., 2016). Factors that likely contribute to these differences include the addition of FGF2 and heparin, the use of BME and the origin of cells (human versus mouse). Other studies did not describe the initial organoid-forming efficiency (Zhang et al., 2016b) or they initiated organoid cultures from tissue fragments (Jardé et al., 2016) or pre-formed 3D colonies (Panciera et al., 2016), rather than single cells. Here, we have discriminated between freshly isolated luminal and basal cells for organoid formation and show that ∼20% of basal cells exhibit stem cell potential, suggesting that the culture conditions recapitulate features of the MaSC niche.

To address whether the organoids derived from single cells, we exploited the multicolor-reporter Confetti mouse model, a powerful

Development (2017) 144, 1065-1071 doi:10.1242/dev.145045

tool for clonal analysis (Rios et al., 2014; Snippert et al., 2010). In the basal model, K5-rtTA/TetO-cre/R26R-Confetti transgenic mice, *cre*-mediated recombination of the floxed 'confetti' locus randomly activates one of four reporter colors. This leads to the marking of recombined K5-expressing stem cells and all progeny for their entire lifespan (Clevers, 2016; Rios et al., 2014). Confetti-marked (GFP/CFP/RFP/YFP) basal cells were isolated by flow cytometry (Fig. S2) and plated at varying cell densities. Confocal fluorescence microscopy revealed the formation of uni-colored clonal organoids, whereas multi-colored polyclonal structures were rarely observed (Fig. 1E,F). This indicates an efficient assay for clonal organoid formation. Importantly, cells of basal-derived organoids maintained their ability to generate mammary ductal trees *in vivo* (Fig. S1E). Recent studies have shown organoid cells can repopulate the mammary fat pad *in vivo* even after prolonged passaging or CRISPR-mediated gene editing (Jardé et al., 2016; Panciera et al., 2016; Zhang et al., 2016b).

Characterization of organoid architecture using 3D confocal imaging

Confocal imaging in 3D was used to examine the cellular composition of the organoids, and revealed that basal-derived organoids contained $K14^+$ and $p63^+$ basal, as well as $K8/18^+$ and E-cadherin$^+$ luminal, cells (Fig. 2A-C). Importantly, the basal/myoepithelial cells displayed their characteristic elongated morphology, remarkably similar to that observed *in vivo* (Rios et al., 2014), and wrapped around buds of cuboidal luminal cells (Fig. 2A,B). Staining for F-actin, a marker of the apical membrane

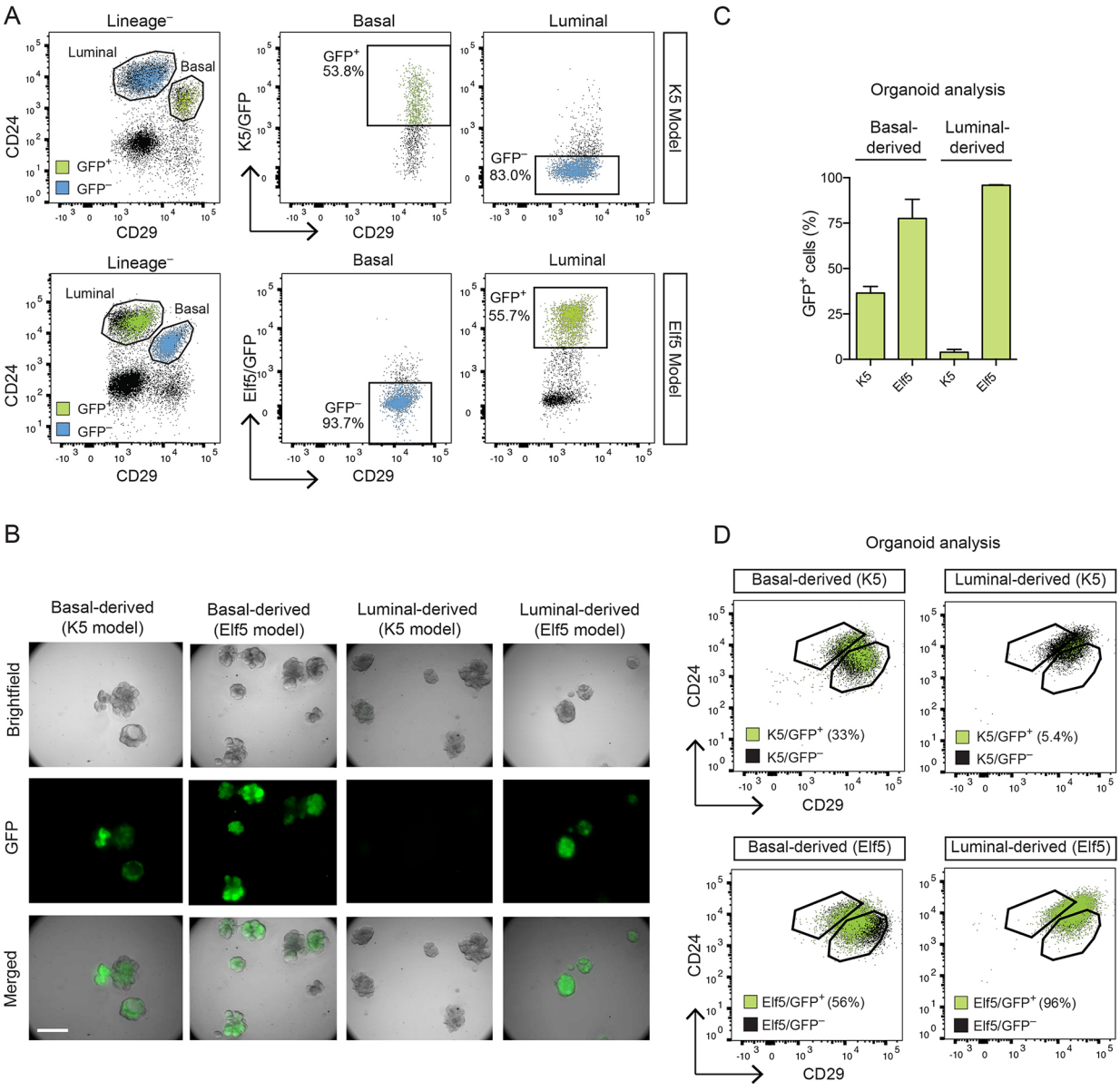

Fig. 3. Analysis of organoids generated from K5- and Elf5-reporter mouse models. (A) FACS plots showing the sorting strategy for Elf5$^-$/GFP$^-$ basal and Elf5$^+$/GFP$^+$ luminal progenitor cells isolated from Elf5-GFP reporter mice, or K5$^+$/GFP$^+$ basal and K5$^-$/GFP$^-$ luminal cells from K5-GFP reporter mice. (B) Representative bright-field and GFP-fluorescent images of organoids derived from either basal cells or luminal cells of GFP reporter mice. Scale bar: 250 µm. (C) Quantification of GFP$^+$ cells by FACS analysis of digested organoids derived from sorted cells (n=2 or 3 experiments). (D) Representative FACS plots showing GFP$^+$ (see C) and GFP$^-$ cell populations from digested basal- and luminal-derived reporter organoids. The gating strategy for luminal and basal populations isolated from control mice is indicated.

Development (2017) 144, 1065-1071 doi:10.1242/dev.145045

in polarized epithelium, revealed that organoids contain regions with a central lumen lined by the apical membrane of luminal cells (Fig. 2C), which is reminiscent of normal ductal architecture (Rios et al., 2014). Although some regions of the organoids comprised bilayered structures, as seen *in vivo*, other inner regions contained multiple layers of luminal cells (Fig. 2B,D), similar to the body region of the terminal end bud (TEB).

Organoids derived from luminal MECs resembled the overall budding architecture of the basal-derived organoids, but were composed of luminal cells. However, rare $K14^+$ basal cells were occasionally evident, suggesting that de-differentiation had occurred (Fig. 2E). This phenomenon may reflect an artefact of cell culture, which has been observed upon long-term culture of luminal cells (Péchoux et al., 1999) and prostate organoids (Karthaus et al., 2014). Many estrogen receptor (ER)-positive cells were detected in basal-derived organoids, consistent with the existence of mature ductal cells (Fig. 2F). Importantly, the lactogenic hormone prolactin induced luminal cells to produce milk that was secreted into the organoid lumen (Fig. 2G). Thus, the mammary organoids retain full functional capability.

Passaging of basal-derived structures by mechanical or mild enzymatic disruption indicated that organoid morphology could be maintained up to at least passage four (Fig. S3). In contrast to mammary organoid passaging via single cells, as previously reported (Jardé et al., 2016; Panciera et al., 2016; Zhang et al., 2016a,b), this method disaggregates organoids into smaller fragments and leaves the bi-layered structures intact.

In vitro lineage tracing of MECs using mouse reporter models

To assess the potential of the organoid culture system for tracking the fate of basal and luminal cells *in vitro*, we used Elf5-rtTA-IRES-GFP and K5-rtTA-IRES-GFP reporter mice, in which expression of GFP is driven by gene promoters specific for either luminal progenitor or basal cells, respectively (Rios et al., 2014). From these, $Elf5^-/GFP^-$ or $K5^+/GFP^+$ basal cells, $Elf5^+/GFP^+$ luminal progenitor cells or $K5^-/GFP^-$ luminal cells were sorted for organoid generation (Fig. 3A).

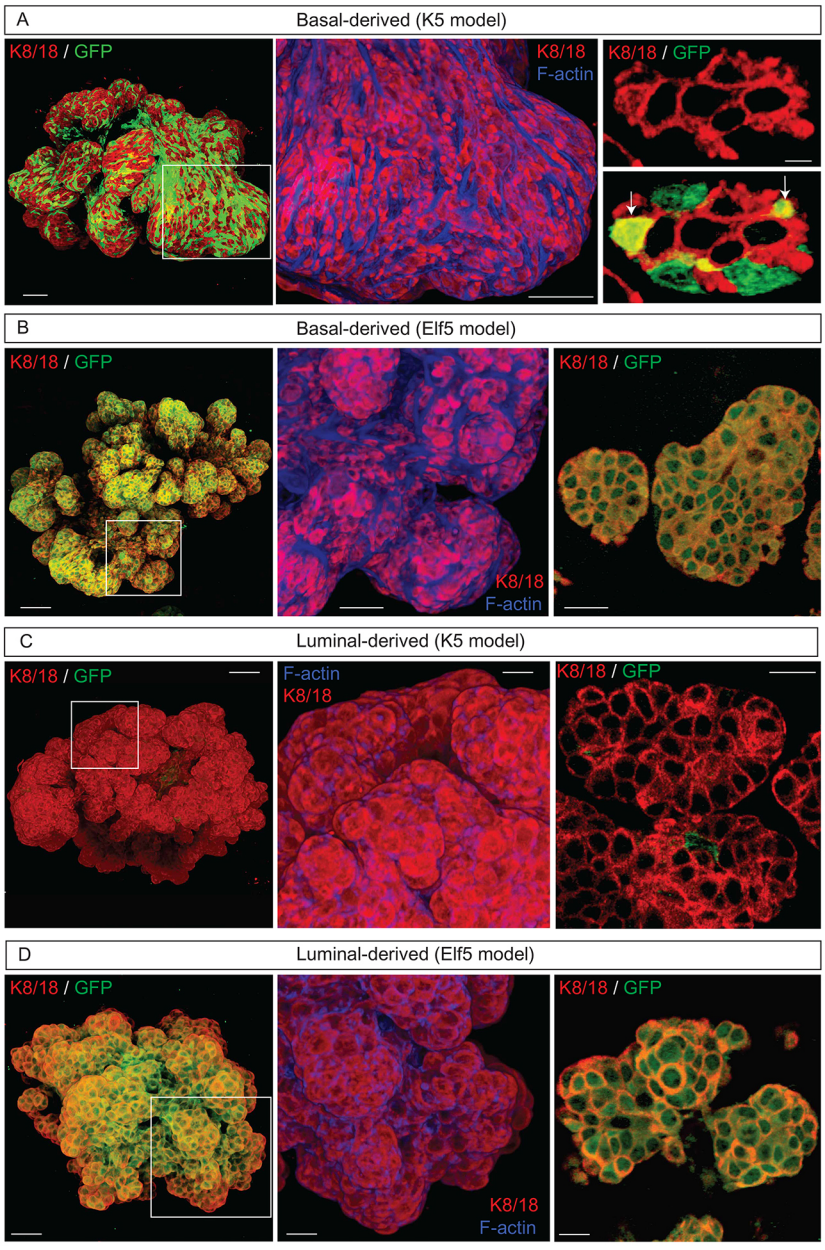

Fig. 4. 3D imaging of organoids generated from K5- and Elf5- reporter mouse models. (A-D) Representative whole-mount 3D confocal images, enlarged sections and optical sections of organoids derived from $K5^+/GFP^+$ basal cells (A), $Elf5^-/GFP^-$ basal cells (B), $K5^-/GFP^-$ luminal cells (C) or $Elf5^+/GFP^+$ luminal progenitor cells (D), sorted from GFP reporter mice, labeled for GFP, K8/18 and F-actin. In A, arrows indicate cells co-staining for GFP and K8/18. Scale bars (from left to right): 30 µm, 30 µm and 5 µm (A); 50 µm, 30 µm and 30 µm (B); 50 µm, 25 µm and 15 µm (C); 30 µm, 20 µm and 20 µm (D). *n*=3 experiments; two to four structures were imaged per experiment.

Development (2017) 144, 1065-1071 doi:10.1242/dev.145045

Wide-field fluorescent imaging revealed that organoids derived from either basal or luminal cells were Elf5$^+$/GFP$^+$, whereas K5$^+$/GFP$^+$ organoids were detected only when cultured from basal and not luminal cells (Fig. 3B). Of note, we found that the Elf5$^-$/GFP$^-$ mature luminal cells did not form organoids (Fig. S4), in accordance with previous studies (Asselin-Labat et al., 2007). A recent study, however, has indicated that mature luminal cells can be reprogrammed to organoid-forming (MaSC-like) cells by activation of YAP/TAZ signaling (Panciera et al., 2016).

To quantitate the proportion of GFP$^+$ cells, organoids were processed into single cells and analyzed by flow cytometry. Organoids derived from K5$^+$/GFP$^+$ or Elf5$^-$/GFP$^-$ basal cells contained 36% or 77% GFP$^+$ cells, respectively (Fig. 3C), indicating that single basal cells can differentiate into basal and luminal cells *in vitro*, compatible with data shown in Fig. 2A. Conversely, the presence of GFP$^+$ cells in organoids generated from K5$^-$/GFP$^-$ (<4%) or Elf5$^+$/GFP$^+$ or (>95%) luminal cells is compatible with the restricted fate of luminal progenitor cells *in vivo* (Fig. 3C) (Rios et al., 2014; Asselin-Labat et al., 2007). Even though the total cell population appears as a homogeneous CD24$^+$CD29$^+$ population following cell culture, as opposed to two distinct populations in the case of freshly isolated cells, flow cytometry indicated that K5$^+$/GFP$^+$ cells and Elf5$^+$/GFP$^+$ cells were closer to the basal and luminal compartments, respectively (Fig. 3D).

High-resolution 3D confocal microscopy was next used to visualize GFP expression at the single cell level (Fig. 4). As expected, we observed that K5$^+$/GFP$^+$ basal cells produced budding structures with an inner layer of K8/18$^+$ luminal cells, surrounded by an outer network of K8/18 negative and GFP$^+$ elongated basal/myoepithelial cells (Fig. 4A). The inner network of K8/K18$^+$ luminal cells in these structures comprised a mix of both GFP$^+$ and GFP$^-$ cells (Fig. 4A), which likely reflects the stability of GFP protein (half-life 24 h). This was further supported by FACS analysis, which indicated that some organoid-derived GFP$^+$ cells lie in the luminal compartment and are negative for K5 expression, whereas GFP$^+$ cells from the basal population stained positive for K5 (Fig. S5). Organoids derived from Elf5$^-$/GFP$^-$ basal cells comprised luminal cells that expressed both GFP and K8/18, and GFP$^-$ and K8/18$^-$ elongated basal/myoepithelial cells (Fig. 4B). Luminal organoids largely maintained their GFP expression (Elf5 derived) or lacked GFP expression when derived from K5-GFP reporter mice, with the exception of rare cells that switched to K5-GFP-expressing cells (Fig. 4C,D). These data demonstrate that the fate of cells harboring K5- or Elf5-specific fluorescent reporter genes can be traced *in vitro* using mammary organoids, and confirm the bipotent capacity of cells within the basal compartment.

In conclusion, we have established a robust method for generating organoids from single basal cells that faithfully mimic the structural and functional features of the bi-layered epithelial tree. Single basal cells could produce progeny that self-organized into 3D ductal structures, encompassing an inner luminal area and outer myoepithelial layer. Cultured cells retained their regenerative capacity, as they were able to form ductal outgrowths *in vivo*. Importantly, myoepithelial cells retained their native morphology under these conditions, a feature that is typically lost in standard Matrigel assays. Furthermore, luminal cells exhibited full functionality, as reflected by their milk-producing capacity. The combination of this mammary organoid system with fluorescent reporter mice was applied to study organoid clonality and track cell fate *in vitro*. This robust mammary organoid model offers a versatile and rapid system for exploring tissue dynamics and mechanisms underlying breast oncogenesis following genetic manipulation using technologies such as CRISPR/Cas9 editing.

MATERIALS AND METHODS

Mice

R26R-Confetti mice were a kind gift from and H. Clevers (Hubrecht Institute, Utrecht, The Netherlands). Elf5-rtTA-IRES-GFP and K5-rtTA-IRES-GFP mice were generated at the Walter and Eliza Hall Institute of Medical Research (WEHI, Parkville, Victoria, Australia) (Rios et al., 2014). FVB/N mice were provided by the WEHI animal facility. For induction of expression of the Confetti reporter in the K5-rtTA/TetO-cre/R26R-Confetti line, mice were injected intraperitoneally with 2 mg of doxycycline (100 ml, 20 mg/ml in PBS; Sigma) over 3 sequential days and collected 4 weeks later. All animal experiments conform to regulatory standards and were approved by the Walter and Eliza Hall Institute (WEHI) Animal Ethics Committee.

Flow cytometry

Fresh inguinal and thoracic mammary glands were dissected from 8- to 12-week-old female mice and single-cell suspensions generated as described previously (Shackleton et al., 2006). Cells were stained with the antibodies listed in Table S2 and sorted on FACS ARIA II (Becton Dickinson). Data were analyzed using FlowJo software.

Organoid culture

Single cells were seeded in basement membrane extract (BME; Cultrex) in uncoated 24-well plates (four drops of 10 µl per well containing 25 cells, for Confetti-fluorescent cells up to 200) and cultured in Advanced DMEM/F12 supplemented with factors listed in Table S1 with or without Wtn3a and R-spondin-2 conditioned medium (Tan et al., 2015; Zhang et al., 2016a), or FGF2 and heparin for 12-14 days. Milk production was induced by incubation with minimal medium with or without prolactin for 48-96 h. ROCK inhibitor (Y27632) was added for the first 3 days and the medium was refreshed every 2-3 days. For organoid proliferation measurements, 25 single cells/10 µl BME were plated in 96-well plates (Nunc). After 12-14 days, CellTiter-Glo Luminescent Cell Viability Assay (Promega) was used to measure cell proliferation. For flow cytometry, 12- to 14-day-old organoids were dissociated into single cells using TrypLE express (Thermo Fisher Scientific) prior to staining (Shackleton et al., 2006). For transplantation assays, 5×10^4 single cells obtained from 12- to 14-day-old organoids were injected into cleared mammary fat pads of 3-week-old FVB recipient mice; the glands harvested after 5 weeks were whole mounted and stained with carmine.

Imaging

BME was dissolved in ice-cold Cell Recovery Solution (Corning) and organoids were then fixed for 30 min in 4% paraformaldehyde, washed with PBT (PBS, 0.1% Tween) and incubated overnight at 4°C with primary antibodies, followed by washing steps and overnight incubation with secondary antibodies (Table S2) (Rios et al., 2014). The following day, organoids were washed and incubated in 80% glycerol for 1 h before 3D imaging using a SP8 confocal microscope. 3D rendering was performed using the Imaris software as described previously (Rios et al., 2014, 2016). Confetti-fluorescent living cultures were imaged as described above, and scored using the 3D visualization module of Imaris.

Statistics

Statistical analysis was performed using GraphPad Prism software using Student's *t*-test.

Acknowledgements

We thank F. Jackling and the animal, FACS, imaging and histology facilities at WEHI for expert assistance; and A. Burgess and N. Kershaw for providing the Rspo2-conditioned medium.

Competing interests

The authors declare no competing or financial interests.

Author contributions

P.R.J. and J.F.D. designed and performed experiments, analyzed data and wrote the manuscript. A.C.R. supported experimental design and 3D imaging. N.Y.F.

generated the mouse reporter models. J.E.V. wrote the manuscript, and J.E.V. and G.J.L. conceptualized the study.

Funding

This work was supported by the Australian National Health and Medical Research Council (NHMRC) (1016701, 1085191 and 1086727); by NHMRC Independent Research Institute Infrastructure Support Scheme (IRIISS); by the Victorian State Government through Victorian Cancer Agency funding and Operational Infrastructure Support; and by the Australian Cancer Research Foundation. J.F.D. is supported by a Marie Skłodowska Curie global individual fellowship of the European Commission. A.C.R. and N.Y.F. were supported by National Breast Cancer Foundation (NBCF)/Cure Cancer Australia Foundation Fellowships; G.J.L. was supported by a NHMRC Fellowship (1078730); and J.E.V. was supported by NHMRC Fellowships (1037230, 1102742).

Supplementary information

Supplementary information available online at
http://dev.biologists.org/lookup/doi/10.1242/dev.145045.supplemental

References

Asselin-Labat, M.-L., Sutherland, K. D., Barker, H., Thomas, R., Shackleton, M., Forrest, N. C., Hartley, L., Robb, L., Grosveld, F. G., van der Wees, J. et al. (2007). Gata-3 is an essential regulator of mammary-gland morphogenesis and luminal-cell differentiation. *Nat. Cell Biol.* **9**, 201-209.

Boj, S. F., Hwang, C.-I., Baker, L. A., Chio, I. I. C., Engle, D. D., Corbo, V., Jager, M., Ponz-Sarvise, M., Tiriac, H., Spector, M. S. et al. (2015). Organoid models of human and mouse ductal pancreatic cancer. *Cell* **160**, 324-338.

Clevers, H. (2016). Modeling development and disease with organoids. *Cell* **165**, 1586-1597.

Ewald, A. J., Brenot, A., Duong, M., Chan, B. S. and Werb, Z. (2008). Collective epithelial migration and cell rearrangements drive mammary branching morphogenesis. *Dev. Cell* **14**, 570-581.

Huch, M., Dorrell, C., Boj, S. F., van Es, J. H., Li, V. S. W., van de Wetering, M., Sato, T., Hamer, K., Sasaki, N., Finegold, M. J. et al. (2013). In vitro expansion of single Lgr5+ liver stem cells induced by Wnt-driven regeneration. *Nature* **494**, 247-250.

Jardé, T., Lloyd-Lewis, B., Thomas, M., Kendrick, H., Melchor, L., Bougaret, L., Watson, P. D., Ewan, K., Smalley, M. J. and Dale, T. C. (2016). Wnt and Neuregulin1/ErbB signalling extends 3D culture of hormone responsive mammary organoids. *Nat. Commun.* **7**, 13207.

Karthaus, W. R., Iaquinta, P. J., Drost, J., Gracanin, A., van Boxtel, R., Wongvipat, J., Dowling, C. M., Gao, D., Begthel, H., Sachs, N. et al. (2014). Identification of multipotent luminal progenitor cells in human prostate organoid cultures. *Cell* **159**, 163-175.

Kim, K.-A., Wagle, M., Tran, K., Zhan, X., Dixon, M. A., Liu, S., Gros, D., Korver, W., Yonkovich, S., Tomasevic, N. et al. (2008). R-Spondin family members regulate the Wnt pathway by a common mechanism. *Mol. Biol. Cell* **19**, 2588-2596.

Linnemann, J. R., Miura, H., Meixner, L. K., Irmler, M., Kloos, U. J., Hirschi, B., Bartsch, H. S., Sass, S., Beckers, J., Theis, F. J. et al. (2015). Quantification of regenerative potential in primary human mammary epithelial cells. *Development* **142**, 3239-3251.

Mroue, R. and Bissell, M. J. (2013). Three-dimensional cultures of mouse mammary epithelial cells. *Methods Mol. Biol.* **945**, 221-250.

Panciera, T., Azzolin, L., Fujimura, A., Di Biagio, D., Frasson, C., Bresolin, S., Soligo, S., Basso, G., Bicciato, S., Rosato, A. et al. (2016). Induction of expandable tissue-specific stem/progenitor cells through transient expression of YAP/TAZ. *Cell Stem Cell* **19**, 725-737.

Péchoux, C., Gudjonsson, T., Rønnov-Jessen, L., Bissell, M. J. and Petersen, O. W. (1999). Human mammary luminal epithelial cells contain progenitors to myoepithelial cells. *Dev. Biol.* **206**, 88-99.

Rios, A. C., Fu, N. Y., Lindeman, G. J. and Visvader, J. E. (2014). In situ identification of bipotent stem cells in the mammary gland. *Nature* **506**, 322-327.

Rios, A. C., Fu, N. Y., Jamieson, P. R., Pal, B., Whitehead, L., Nicholas, K. R., Lindeman, G. J. and Visvader, J. E. (2016). Essential role for a novel population of binucleated mammary epithelial cells in lactation. *Nat. Commun.* **7**, 11400.

Sato, T., Vries, R. G., Snippert, H. J., van de Wetering, M., Barker, N., Stange, D. E., van Es, J. H., Abo, A., Kujala, P., Peters, P. J. et al. (2009). Single Lgr5 stem cells build crypt-villus structures in vitro without a mesenchymal niche. *Nature* **459**, 262-265.

Sato, T., Stange, D. E., Ferrante, M., Vries, R. G. J., van Es, J. H., van den Brink, S., van Houdt, W. J., Pronk, A., van Gorp, J., Siersema, P. D. et al. (2011a). Long-term expansion of epithelial organoids from human colon, adenoma, adenocarcinoma, and Barrett's epithelium. *Gastroenterology* **141**, 1762-1772.

Sato, T., van Es, J. H., Snippert, H. J., Stange, D. E., Vries, R. G., van den Born, M., Barker, N., Shroyer, N. F., van de Wetering, M. and Clevers, H. (2011b). Paneth cells constitute the niche for Lgr5 stem cells in intestinal crypts. *Nature* **469**, 415-418.

Shackleton, M., Vaillant, F., Simpson, K. J., Stingl, J., Smyth, G. K., Asselin-Labat, M.-L., Wu, L., Lindeman, G. J. and Visvader, J. E. (2006). Generation of a functional mammary gland from a single stem cell. *Nature* **439**, 84-88.

Snippert, H. J., van der Flier, L. G., Sato, T., van Es, J. H., van den Born, M., Kroon-Veenboer, C., Barker, N., Klein, A. M., van Rheenen, J., Simons, B. D. et al. (2010). Intestinal crypt homeostasis results from neutral competition between symmetrically dividing Lgr5 stem cells. *Cell* **143**, 134-144.

Sokol, E. S., Miller, D. H., Breggia, A., Spencer, K. C., Arendt, L. M. and Gupta, P. B. (2016). Growth of human breast tissues from patient cells in 3D hydrogel scaffolds. *Breast Cancer Res.* **18**, 19.

Stingl, J., Eaves, C. J., Kuusk, U. and Emerman, J. T. (1998). Phenotypic and functional characterization in vitro of a multipotent epithelial cell present in the normal adult human breast. *Differentiation* **63**, 201-213.

Stingl, J., Eaves, C. J., Zandieh, I. and Emerman, J. T. (2001). Characterization of bipotent mammary epithelial progenitor cells in normal adult human breast tissue. *Breast Cancer Res. Treat.* **67**, 93-109.

Stingl, J., Eirew, P., Ricketson, I., Shackleton, M., Vaillant, F., Choi, D., Li, H. I. and Eaves, C. J. (2006). Purification and unique properties of mammary epithelial stem cells. *Nature* **439**, 993-997.

Tan, C. W., Hirokawa, Y. and Burgess, A. W. (2015). Analysis of Wnt signalling dynamics during colon crypt development in 3D culture. *Sci. Rep.* **5**, 11036.

van Amerongen, R., Bowman, A. N. and Nusse, R. (2012). Developmental stage and time dictate the fate of Wnt/β-catenin-responsive stem cells in the mammary gland. *Cell Stem Cell* **11**, 387-400.

van de Wetering, M., Francies, H. E., Francis, J. M., Bounova, G., Iorio, F., Pronk, A., van Houdt, W., van Gorp, J., Taylor-Weiner, A., Kester, L. et al. (2015). Prospective derivation of a living organoid biobank of colorectal cancer patients. *Cell* **161**, 933-945.

Van Keymeulen, A., Rocha, A. S., Ousset, M., Beck, B., Bouvencourt, G., Rock, J., Sharma, N., Dekoninck, S. and Blanpain, C. (2011). Distinct stem cells contribute to mammary gland development and maintenance. *Nature* **479**, 189-193.

Wang, D., Cai, C., Dong, X., Yu, Q. C., Zhang, X.-O., Yang, L. and Zeng, Y. A. (2015). Identification of multipotent mammary stem cells by protein C receptor expression. *Nature* **517**, 81-84.

Watanabe, K., Ueno, M., Kamiya, D., Nishiyama, A., Matsumura, M., Wataya, T., Takahashi, J. B., Nishikawa, S., Nishikawa, S.-I., Muguruma, K. et al. (2007). A ROCK inhibitor permits survival of dissociated human embryonic stem cells. *Nat. Biotechnol.* **25**, 681-686.

Watson, C. J. and Khaled, W. T. (2008). Mammary development in the embryo and adult: a journey of morphogenesis and commitment. *Development* **135**, 995-1003.

Zeng, Y. A. and Nusse, R. (2010). Wnt proteins are self-renewal factors for mammary stem cells and promote their long-term expansion in culture. *Cell Stem Cell* **6**, 568-577.

Zhang, L., Adileh, M., Martin, M. L., Klingler, S., White, J., Ma, X., Howe, L. R., Brown, A. M. C. and Kolesnick, R. (2016a). Establishing estrogen-responsive mouse mammary organoids from single Lgr5+ cells. *Cell Signal.* **29**, 41-51.

Zhang, Z., Christin, J. R., Wang, C., Ge, K., Oktay, M. H. and Guo, W. (2016b). Mammary-stem-cell-based somatic mouse models reveal breast cancer drivers causing cell fate dysregulation. *Cell Rep.* **16**, 3146-3156.